Original Research

Comparison of Gadobenate Dimeglumine-Enhanced Breast MRI and Gadopentetate Dimeglumine-Enhanced Breast MRI With Mammography and Ultrasound for the Detection of Breast Cancer

Fiona J. Gilbert, MD,[1]* Harrie C.M. van den Bosch, MD,[2] Antonella Petrillo, MD,[3] Katja Siegmann, MD,[4] Johannes T. Heverhagen, MD,[5] Pietro Panizza, MD,[6] Hans-Björn Gehl, MD,[7] Federica Pediconi, MD,[8] Felix Diekmann, MD,[9] Wei-Jun Peng, MD,[10] Lin Ma, MD,[11] Francesco Sardanelli, MD,[12] Paolo Belli, MD,[13] Stefano Corcione, MD,[14] Christian M. Zechmann, MD,[15] Matthieu Faivre-Pierret, MD,[16] and Laura Martincich, MD[17]

Purpose: To compare gadobenate dimeglumine-enhanced magnetic resonance imaging (MRI) with gadopentetate dimeglumine-enhanced MRI, mammography, and ultrasound for breast cancer detection across different malignant lesion types and across different densities of breast tissue.

Materials and Methods: In all, 153 women with Breast Imaging Reporting and Data System (BI-RADS) 3–5 findings on mammography and/or ultrasound underwent identical breast MRI exams at 1.5T with gadobenate dimeglumine and gadopentetate dimeglumine. Images were evaluated by three independent blinded radiologists. Mammography, ultrasound, and combined mammography and/or ultrasound findings were available for 108, 109, and 131 women. Imaging findings were matched with histology data by a fourth, independent, blinded radiologist. Malignant lesion detection rates and diagnostic performance were compared.

Results: In all, 120, 120, and 140 confirmed malignant lesions were present in patients undergoing MRI+mammography, MRI+ultrasound, and MRI+mammography and/or ultrasound, respectively. Significantly greater cancer detection rates were noted by all three readers for comparisons of gadobenate dimeglumine-enhanced MRI with mammography (Δ15.8–17.5%; $P < 0.0001$), ultrasound (Δ18.3–20.0%; $P < 0.0001$), and mammography and/or ultrasound (Δ8.6–10.7%; $P \leq 0.0105$) but not for comparisons of gadopentetate dimeglumine-enhanced MRI with conventional techniques ($P > 0.05$). The false-positive detection rates were lower on gadobenate dimeglumine-enhanced MRI than on conventional imaging (4.0–5.5% vs. 11.1% at mammography; 6.3–8.4% vs. 15.5% at ultrasound). Significantly

[1]University Department of Radiology, University of Cambridge, Cambridge, UK.
[2]Department of Radiology, Catharina Hospital, Eindhoven, The Netherlands.
[3]Division of Diagnostic Imaging, Department of Diagnostic Imaging, Radiant and Metabolic Therapy, "Istituto Nazionale dei Tumori Fondazione G. Pascale" – IRCCS, Naples, Italy.
[4]Department of Diagnostic and Interventional Radiology, University Hospital Tuebingen, Tuebingen, Germany.
[5]Department of Diagnostic Radiology, University Hospital, Philipps University, Marburg, Germany.
[6]Department of Radiology, Scientific Institute, Ospedale San Raffaele, Milan, Italy.
[7]Department of Diagnostic and Interventional Radiology, Klinikum Bielefeld, Academic Teaching Hospital University of Münster, Bielefeld, Germany.
[8]Department of Radiological Sciences, University of Rome "La Sapienza," Rome, Italy.
[9]Department of Radiology, Institut für Radiologie, Charité-Universitätsmedizin, Berlin, Germany.
[10]Radiology Department, Cancer Hospital, Fudan University, Shanghai, P.R. China.
[11]Department of Radiology, Chinese People's Liberation Army (PLA) General Hospital, Beijing, P.R. China.
[12]Università degli Studi di Milano, Dipartimento di Scienze Biomediche per la Salute, Unità di Radiologia, IRCCS Policlinico San Donato, San Donato Milanese, Milan, Italy.
[13]Department of Bioimaging and Radiological Sciences, Institute of Radiology, "A. Gemelli" Hospital - Catholic University, Rome, Italy.
[14]Senology Unit, University Hospital "S. Anna," Ferrara, Italy.
[15]Department of Radiology, German Cancer Research Center, Heidelberg, Germany.
[16]Department of Radiology, Center Oscar Lambret, Lille, France.
[17]Department of Diagnostic Imaging, Institute for Cancer Research and Treatment (IRCC), Candiolo, Torino, Italy.
*Address reprint requests to: F.J.G., University Department of Radiology, Box 218, Level 5, Addenbrooke's Hospital, Hills Road, Cambridge CB2 0QQ, UK. E-mail: fjg28@medschl.cam.ac.uk

Received May 9, 2013; Accepted July 30, 2013.
DOI 10.1002/jmri.24434
View this article online at wileyonlinelibrary.com.

improved cancer detection on MRI was noted in heterogeneously dense breast (91.2–97.3% on gadobenate dimeglumine-enhanced MRI vs. 77.2–84.9% on gadopentetate dimeglumine-enhanced MRI vs. 71.9-84.9% with conventional techniques) and for invasive cancers (93.2–96.2% for invasive ductal carcinoma [IDC] on gadobenate dimeglumine-enhanced MRI vs. 79.7–88.5% on gadopentetate dimeglumine-enhanced MRI vs. 77.0–84.4% with conventional techniques). Overall diagnostic performance for the detection of cancer was superior on gadobenate dimeglumine-enhanced MRI than on conventional imaging or gadopentetate dimeglumine-enhanced MRI.

Conclusion: Gadobenate dimeglumine-enhanced MRI significantly improves cancer detection compared to gadopentetate dimeglumine-enhanced MRI, mammography, and ultrasound in a selected group of patients undergoing breast MRI for preoperative staging or because of inconclusive findings at conventional imaging.

Key Words: breast cancer; gadobenate dimeglumine-enhanced MRI; mammography; ultrasound
J. Magn. Reson. Imaging 2013;00:000–000.

SELECTION OF THE APPROPRIATE MANAGEMENT OPTION for patients with confirmed breast cancer depends on accurate determination of the full extent of disease (1–3). Of the techniques available, magnetic resonance imaging (MRI) is considered superior to conventional imaging techniques for cancer detection (4–11). This has led to the increased use of breast MRI in patient management. However, there is concern about the relatively low specificity, particularly in preoperative staging of the breast, which can lead to unnecessary biopsies or even mastectomy (12). There is a pressing need to improve diagnostic performance through improved image resolution and better lesion delineation.

Recently, a large-scale, prospective, multicenter, intraindividual clinical trial (DETECT (13)) confirmed the results of two prior single-center studies (14,15) in showing superiority for MRI enhanced with gadobenate dimeglumine (MultiHance; Bracco Imaging SpA, Milan, Italy) as compared with MRI enhanced with gadopentetate dimeglumine (Magnevist; Bayer Healthcare, Berlin, Germany) for the detection breast cancer.

The present analysis compares gadobenate dimeglumine-enhanced MRI with gadopentetate dimeglumine-enhanced MRI, mammography, and ultrasound for breast cancer detection across different malignant lesion types and across different densities of breast tissue.

MATERIALS AND METHODS

Patients

The DETECT study (13) was performed at 17 sites in Europe and China between July 2007 and May 2009 and evaluated 162 women with an abnormality at mammography or ultrasound that was considered category 3, 4, or 5 for suspicion of malignancy according to the American College of Radiology (ACR) Breast Imaging Reporting and Data System (BI-RADS) classification (16). Patients with congestive heart failure (NYHA classification IV) or a known allergy to either contrast agent were ineligible. Patients were also ineligible if they had received or were scheduled to receive another contrast medium within 24 hours before or after either of the examinations, any other investigational compound and/or medical device within 30 days before until 24 hours after administration of the second agent, or were scheduled to undergo any intervention between the two examinations. Finally, patients were ineligible if they were pregnant or lactating or had any medical condition or other circumstance (eg, metallic vascular stent, pacemaker, severe claustrophobia) that would decrease the chances of obtaining an adequate examination or which would preclude proximity to a strong magnetic field. Institutional Review Board and regulatory approval was granted from each site and all patients provided written consent.

Overall, 153 women (mean age: 52.6 ± 12.3 years) underwent both MRI exams and had on-site final diagnosis (truth standard) data (ie, patient profiles, original mammography and/or ultrasound, and histopathology/surgical reports) available. These 153 women included 123 (80.4%) women who had technically adequate initial mammography results available and 129 (84.3%) women who had technically adequate initial ultrasound results available.

MRI

The 153 evaluable women underwent MRI at 1.5T using commercially available scanners (Siemens Sonata [$n = 19$], Avanto [$n = 15$], Symphony [$n = 15$], Siemens Medical Solutions, Erlangen, Germany; Philips Achieva [$n = 27$], Intera [$n = 28$]; Philips Medical Systems, Best, The Netherlands; GE Signa Excite [$n = 41$], Genesis Signa [$n = 8$]; GE Medical Systems, Milwaukee, WI) equipped with power gradients of at least 30 mT/m. All examinations were performed with the subject in the prone position using a dedicated double breast coil.

Patients were randomized to receive either gadobenate dimeglumine or gadopentetate dimeglumine for the first MRI examination and then the other agent for the second examination after an interval of >48 hours but <7 days to ensure full comparability between examinations. The contrast agent dose (0.1 mmol/kg [0.2 mL/kg] body weight followed by a 20-mL saline flush), injection rate, and mode of injection were identical for both examinations in each patient. Overall, 149 women received contrast agent intravenously by power injector (2 mL/sec in 130 women, 1.8 mL/sec in two women, 1.5 mL/sec in 17 women) while four women received contrast agent as a manual bolus (1–2 mL/sec for ~10 sec ensuring that the same rate was used for both examinations).

The two MRI examinations in each patient were identical in terms of orientation, sequence parameters, and spatial resolution. A standardized protocol comprising a T2-weighted sequence and a 3D T1-weighted gradient-echo (T1wGRE) sequence before contrast agent injection and a series of at least five

T1wGRE sequences at intervals of ≤2 min after contrast injection (beginning at the start of injection; t = 0 min) was used for both examinations in all patients. The pre- and postinjection T1wGRE sequences in each patient were acquired with identical imaging parameters (TR: 4.11–15 msec, TE: 1.35–4.76 msec, flip angle: 10–30°, 1 or 2 excitations, slice thickness: 1.0–2.5 mm with no interslice gap, matrix: >192 × 256, in-plane spatial resolution: ≤1.5 mm^2). A rectangular field-of-view of ≤36 cm covered the whole breast in all cases. The acquisition time was ≤120 seconds for each temporal frame. Fat-suppressed sequences (VIBRANT; GE Healthcare) were used in 32 patients. The unenhanced T2-weighted sequence was acquired with TR: 3000–10,000 msec, TE: 50–140 msec, 1 to 3 excitations, slice thickness: 2.4–3 mm with no interslice gap, matrix: >256 × 256, spatial resolution: >1 × 1 × 2.5 mm, and acquisition time: ≤240 seconds.

MR Image Evaluation

All MR images were evaluated independently by three experienced (5–10 years in breast MRI) radiologists (CMZ, MFP, LM) who were unaffiliated with the study centers and fully blinded to the contrast agent used in each examination, to all patient clinical and radiological information, and to all interpretations by on-site investigators. Images were presented for review on a multimonitor imaging workstation (TeraRecon AquariusNet server v. 4.4.1.4; San Mateo, CA). All routine image processing functions (eg, window/level, zoom, pan) were available.

Detected lesions were classified as malignant or benign on the basis of lesion morphology using the BI-RADS MRI classification for suspicion of malignancy (16) and by assessing postcontrast signal intensity–time curves obtained at regions of interest positioned on lesion areas with the strongest and fastest enhancement (13). The signal intensity–time curves were classified according to shape, from type I to type III as described elsewhere (17,18). Lesions scored as BI-RADS 3, 4, or 5 were considered suspicious and were included in the analysis. For the purposes of this analysis lobular carcinoma in situ (LCIS) was considered a benign lesion.

All identified mass lesions were numbered and the location recorded on image screenshots by breast region (10 regions per patient: right/left superior lateral, superior medial, inferior medial, inferior lateral, central/subareolar) for subsequent matching with on-site truth standard data. The size (≤5 mm, 6–10 mm, 11–20 mm, >20 mm), shape (round, oval, lobular, irregular), and margins (smooth/well-defined, lobulated, irregular/ill-defined, spiculated) of identified lesions were recorded to aid lesion matching.

Conventional Imaging

All patients included in this analysis underwent x-ray mammography, breast ultrasound, or both within 30 days before the first breast MRI examination. Minimally, at least two orthogonal views of the breast were obtained for each imaging study in order to diagnose and locate a lesion.

Mammography

Conventional x-ray mammograms were acquired using equipment from established manufacturers. Of the 123 women with mammograms, 68 underwent digital mammography while 55 underwent conventional film mammography. In all cases a mediolateral oblique view and a craniocaudal view were obtained according to the standard clinical practice in place at the investigating center.

Ultrasound

Breast ultrasound was performed in 129 women using ultrasound equipment from established manufacturers at transducer frequencies of between 7.5 and 17.5 MHz (typically between 10 and 15 MHz). The ultrasound approaches employed varied with the investigating center according to the standard clinical practice in place but typically included cross-sectional fundamental and harmonic techniques, power Doppler and color Doppler techniques, and 3D radial scanning techniques.

Assessment of X-ray Mammography and Breast Ultrasound Images

X-ray mammography and ultrasound procedures were performed and reviewed by on-site investigators (FJG, HCMvdB, AP, KS, JTH, PP, HBG, FP, FD, WJP, LM, FS, PB; each with ≥10 years in diagnostic breast imaging) according to the standard clinical practice at each individual site. Lesions identified at mammography and ultrasound were numbered and labeled by the on-site investigator who performed the examination using identical breast maps to those used subsequently by the off-site blinded readers of MR images. Assessment of lesion nature based on mammogram and ultrasound images was carried out as performed routinely using the BI-RADS mammography and ultrasound final assessment categories (16).

Breast Density

Determination of breast tissue density was performed for all patients who underwent mammography. Tissue density was classified using the BI-RADS classification scheme (16) as 1) almost entirely fatty (<25% glandular); 2) containing scattered fibroglandular densities (25–50% glandular); 3) heterogeneously dense (51–75% glandular); or 4) extremely dense (>75% glandular).

Lesion Matching

After all image sets had been evaluated, a lesion matching session was performed. This evaluation was performed by an independent, reviewer (SC; 20 years of experience in breast imaging) who was not involved in either the on-site conduct of the study or the off-site assessment of MR images.

Lesion matching was performed to match any lesions seen on the breast maps produced by the on-site investigators with lesions detected independently by the three off-site readers of MR images. Only lesion maps were viewed during this session (ie, no ultrasound, mammographic, or breast MR images were displayed at any time). The information provided for each lesion included only location (breast segment) and size. Lesion matching was performed for each off-site blinded reader separately; matching between off-site reviewers was not performed.

Statistical Analysis

Comparison of MRI findings with findings from conventional imaging was performed in terms of the detection of individual histologically confirmed malignant lesions (cancer detection rate: number of malignant lesions at diagnostic imaging/number of malignant lesions confirmed at histology) and by breast region in terms of diagnostic performance (sensitivity, specificity, accuracy, and 95% confidence intervals [CI]; and positive and negative predictive values [PPV, NPV]) for the diagnosis of breast cancer. The former analysis was performed for all histologically confirmed malignant lesions combined and separately by individual lesion type. Comparison of the cancer detection rate was also performed across different categories of breast tissue density. For the latter analysis a breast region with at least one confirmed malignant lesion was considered true positive (TP) while a region without a malignant lesion (no lesion or a confirmed benign lesion) was true negative (TN). Technically inadequate images were considered false negative (FN) if the region was confirmed as malignant or false positive (FP) if the region was normal or benign. Differences in sensitivity, specificity, and accuracy were compared using McNemar's test. Differences in PPV and NPV were compared using the Wald test derived from generalized estimating equations (GEE) with exchangeable working correlation structure. All statistical tests were 2-sided at the $P < 0.05$ level of significance and were performed using SAS v. 8.2 (Cary, NC).

RESULTS

Malignant Lesion Detection

Overall, 108/123 women (52.7 ± 12.7 years) who underwent MRI+mammography, 109/129 women (52.8 ± 13.2 years) who underwent MRI+ultrasound, and 131/153 women (52.6 ± 12.6 years) who underwent MRI+mammography and/or ultrasound had histological confirmation of malignant disease. A total of 120 histologically confirmed malignant lesions (78 invasive ductal carcinomas [IDC] in 63 patients, 24 invasive lobular carcinomas [ILC] in 17 patients, 7 "other" invasive carcinomas [two tubular, two scirrous, one cribriform, one mixed, and one unknown] in five patients, 11 ductal carcinoma in situ [DCIS] in nine patients) were present in the 108 patients who underwent breast MRI and mammography. Likewise, 120 histologically confirmed malignant lesions (74 IDC in 57 patients, 27 ILC in 19 patients, 7 "other" invasive carcinomas in 5 patients, 12 DCIS in 9 patients) were present in the 109 patients who underwent breast MRI and ultrasound. Finally, 140 histologically confirmed malignant lesions (90 IDC in 73 patients, 29 ILC in 21 patients, 7 "other" invasive carcinomas in 5 patients, 14 DCIS in 11 patients) were present in the 131 patients that underwent breast MRI and mammography and/or ultrasound.

The malignant lesion detection rates on MRI enhanced with gadobenate dimeglumine and gadopentetate dimeglumine relative to mammography, ultrasound, and mammography+ultrasound, as well as comparisons between the two MRI examinations, are presented in Fig. 1. Highly significant superiority for MRI enhanced with gadobenate dimeglumine was reported by each reader for comparisons with mammography (Δ15.8–17.5%; $P \leq 0.0001$; Fig. 1a, ultrasound (Δ18.3–20.0%; $P \leq 0.0001$; Fig. 1b), and mammography and/or ultrasound (Δ8.6–10.7%; $P \leq 0.0105$; Fig. 1c). Conversely, no reader reported significant superiority for gadopentetate dimeglumine-enhanced MRI compared to mammography, ultrasound, or mammography and/or ultrasound. Notably, the cancer detection rate on gadopentetate dimeglumine-enhanced MRI was nonsignificantly inferior to that of mammography and/or ultrasound for two readers and equivalent for the third. Findings for comparisons between the two MRI examinations in each patient population reflect findings reported previously (13).

More FN and FP lesions were reported after gadopentetate dimeglumine than after gadobenate dimeglumine by all readers for all three patient populations (Table 1). Although the FP detection rates on MRI were typically lower than those reported for conventional techniques, two of three readers reported a higher FP detection rate for gadopentetate dimeglumine-enhanced MRI than for combined mammography and/or ultrasound.

Lesion Type

Gadobenate dimeglumine-enhanced MRI was superior to gadopentetate dimeglumine-enhanced MRI, mammography, ultrasound, and combined mammography and/or ultrasound for detection of both invasive and noninvasive malignant lesions (Table 2). Significantly superior detection rates with gadobenate dimeglumine were noted for all IDC and most ILC comparisons. For other lesion types the relatively small numbers of lesions precluded demonstration of statistical significance.

Breast Density

The superiority of gadobenate dimeglumine-enhanced MRI was independent of the density of breast tissue (Table 3). Each of the three blinded readers detected more histologically confirmed malignant lesions in each of the four breast density categories apart from in extremely dense breasts in which only six malignant lesions were present. Significant superiority for gadobenate dimeglumine-enhanced MRI versus gadopentetate dimeglumine-enhanced MRI and all comparator techniques was demonstrated in heterogeneously

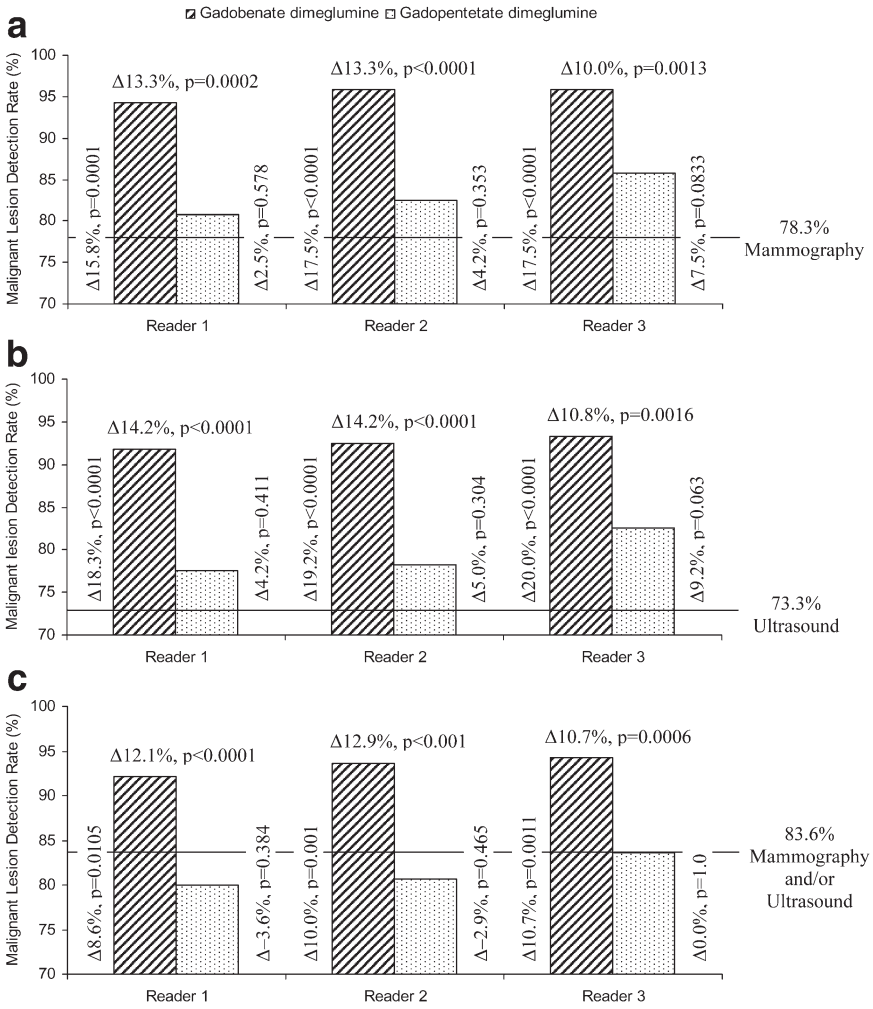

Figure 1. Cancer detection rate on gadobenate dimeglumine-enhanced MRI versus gadopentetate dimeglumine-enhanced MRI relative to mammography (**a**), ultrasound (**b**), and combined mammography and/or ultrasound (**c**).

dense breast tissue in which sufficient numbers of lesions permitted statistical testing. In less dense breasts (0–50% glandular) gadobenate dimeglumine-enhanced MRI detected all malignant lesions present. Conversely, gadopentetate dimeglumine-enhanced MRI detected fewer malignant lesions than mammography in almost entirely fat breasts and was only marginally superior to mammography in slightly denser breasts (25–50% glandular). Examples of malignant lesion detection in breasts with tissue parenchyma of different density are shown in Figs. 2, 3 and 4.

Lesions Detected Only on MRI

Overall, readers 1, 2, and 3 detected 15, 14 and 15 additional histologically confirmed malignant lesions

Table 1
Numbers of False Negative and False Positive Lesions and Comparison of False Positive Detection Rates (FPR)

		Reader 1		Reader 2		Reader 3		
Comparator		Gadobenate dimeglumine	Gadopentetate dimeglumine	Gadobenate dimeglumine	Gadopentetate dimeglumine	Gadobenate dimeglumine	Gadopentetate dimeglumine	Conventional technique
Mammography ($n = 120$)	FN lesions	7	23	5	21	5	17	26
	FP lesions	6	9	7	13	5	18	15
	FPR	4.8% (6/126)	7.0% (9/129)	5.5% (7/127)	9.8% (13/133)	4.0% (5/125)	13.0% (18/138)	11.1% (15/135)
Ultrasound ($n = 120$)	FN lesions	10	27	9	26	8	21	32
	FP lesions	8	13	10	16	11	21	22
	FPR	6.3% (8/128)	9.8% (13/133)	7.7% (10/130)	11.8% (16/136)	8.4% (11/131)	14.9% (21/141)	15.5% (22/142)
Mammography + Ultrasound ($n = 140$)	FN lesions	11	28	9	27	8	23	23
	FP lesions	8	13	11	17	11	24	15
	FPR	5.4% (8/148)	8.5% (13/153)	7.3% (11/151)	10.8% (17/157)	7.3% (11/151)	14.6% (24/164)	9.7% (15/155)

Table 2
Malignant Lesion Detection Rates by Lesion Histological Type

Comparator imaging technique	Reader	Invasive ductal carcinoma (IDC)			Invasive lobular carcinoma (ILC)			Ductal carcinoma in situ (DCIS)[a]		
		Gadobenate dimeglumine	Gadopentetate dimeglumine	Comparator technique	Gadobenate dimeglumine	Gadopentetate dimeglumine	Comparator technique	Gadobenate dimeglumine	Gadopentetate dimeglumine	Comparator technique
Mammography	1	96.2% (75/78)[b,c]	83.3% (65/78)	80.8% (63/78)	100% (24/24)[b,c]	79.2% (19/24)	66.7% (16/24)	81.8% (9/11)	72.7% (8/11)	81.8% (9/11)
	2	94.9% (74/78)[b,c]	84.6% (66/78)		100% (24/24)[b,c]	83.3% (20/24)		90.9% (10/11)	72.7% (8/11)	
	3	96.2% (75/78)[b,c]	88.5% (69/78)		91.7% (22/24)[c]	87.5% (21/24)		100% (11/11)	72.7% (8/11)	
Ultrasound	1	93.2% (69/74)[b,c]	79.7% (59/74)	77.0% (57/74)	100% (27/27)[b,c]	77.8% (21/27)	77.8% (21/27)	75.0% (9/12)	66.7% (8/12)	50.0% (6/12)
	2	93.2% (69/74)[b,c]	81.1% (60/74)		100% (27/27)[b,c]	81.5% (22/27)		66.7% (8/12)	58.3% (7/12)	
	3	94.6% (70/74)[b,c]	85.1% (63/74)		92.6% (25/27)	77.8% (21/27)		83.3% (10/12)[c]	83.3% (10/12)[c]	
Mammography + Ultrasound	1	94.4% (85/90)[b,c]	83.3% (75/90)	84.4% (76/90)	100% (29/29)[b,c]	79.3% (23/29)	82.8% (24/29)	71.4% (10/14)	64.3% (9/14)	71.4% (10/14)
	2	94.4% (85/90)[b,c]	84.4% (76/90)		100% (29/29)[b,c]	82.8% (24/29)		71.4% (10/14)	57.1% (8/14)	
	3	95.6% (86/90)[b,c]	87.8% (79/90)		93.1% (27/29)	79.3% (23/29)		85.7% (12/14)	71.4% (10/14)	

Includes all subjects who had all exams and histology results available and had histologically confirmed malignant lesions.
Numbers in parentheses indicate TP lesions detected at MRI or conventional imaging / total number of histologically confirmed malignant lesions in relevant patient population.
[a]Includes also one lesion categorized as DCIS+LCIS.
[b]Significantly superior malignant lesion detection rate for gadobenate dimeglumine – enhanced MRI compared to gadopentetate dimeglumine – enhanced MRI based on *P*-value when calculable ($P < 0.015$ all evaluations; McNemar's test) or confidence intervals (estimated using paired binary approach) when *P*-value not calculable.
[c]Significantly superior malignant lesion detection rate for MRI compared to comparator imaging technique based on *P*-value when calculable ($P < 0.05$ all evaluations; McNemar's test) or confidence intervals (estimated using paired binary approach) when *P*-value not calculable.

Table 3
Malignant Lesion Detection Rates by Breast Tissue Density

Comparator imaging technique	Reader	Almost entirely fat (<25% glandular)			Scattered islands of fibroglandular density (25–50% glandular)			Heterogenously dense breast (51–75% glandular)			Extremely dense breast (>75% glandular)		
		Gadobenate dimeglumine	Gadopentetate dimeglumine	Comparator technique	Gadobenate dimeglumine	Gadopentetate dimeglumine	Comparator technique	Gadobenate dimeglumine	Gadopentetate dimeglumine	Comparator technique	Gadobenate dimeglumine	Gadopentetate dimeglumine	Comparator technique
Mammography	1	100% (9/9)	77.8% (7/9)	100% (9/9)	100% (32/32)	87.5% (28/32)	84.4% (27/32)	94.5% (69/73)[b,c]	80.8% (59/73)	79.5% (58/73)	50% (3/6)	50% (3/6)	0% (0/6)
(120 lesions)	2	100% (9/9)	77.8% (7/9)		100% (32/32)	87.5% (28/32)		97.3% (71/73)[b,c]	83.6% (61/73)		50% (3/6)	50% (3/6)	
	3	100% (9/9)	88.9% (8/9)		100% (32/32)	96.9% (31/32)		93.2% (68/73)[b,c]	84.9% (62/73)		100% (6/6)	33.3% (2/6)	
Ultrasound[a]	1	100% (8/8)	75.0% (6/8)	62.5% (5/8)	100% (29/29)	86.2% (25/29)	86.2% (25/29)	94.7% (54/57)[b,c]	77.2% (44/57)	71.9% (41/57)	50% (3/6)	50% (3/6)	50% (3/6)
(100 lesions)	2	100% (8/8)	75.0% (6/8)		100% (29/29)	86.2% (25/29)		96.5% (55/57)[b,c]	80.7% (46/57)		50% (3/6)	50% (3/6)	
	3	100% (8/8)	87.5% (7/8)		100% (29/29)	96.6% (28/29)		91.2% (52/57)[c]	84.2% (48/57)		100% (6/6)	33.3% (2/6)	
Mammography +	1	100% (9/9)	77.8% (7/9)	100% (9/9)	100% (32/32)	87.5% (28/32)	90.6% (29/32)	94.5% (69/73)[b]	80.8% (59/73)	84.9% (62/73)	50% (3/6)	50% (3/6)	50% (3/6)
Ultrasound	2	100% (9/9)	77.8% (7/9)		100% (32/32)	87.5% (28/32)		97.3% (71/73)[b,c]	83.6% (61/73)		50% (3/6)	50% (3/6)	
(120 lesions)	3	100% (9/9)	88.9% (8/9)		100% (32/32)	96.9% (31/32)		93.2% (68/73)[b]	84.9% (62/73)		100% (6/6)	33.3% (2/6)	

Includes all subjects who had all exams and histology results available and had histologically confirmed malignant lesions.
Numbers in parentheses indicate TP lesions detected at MRI or conventional imaging / total number of histologically confirmed malignant lesions in relevant patient population.
[a]Includes only patients with available mammographically determined breast tissue density data.
[b]Significantly superior malignant lesion detection rate for gadobenate dimeglumine – enhanced MRI compared to gadopentetate dimeglumine – enhanced MRI based on p-value when calculable ($P < 0.035$ all evaluations; McNemar's test).
[c]Significantly superior malignant lesion detection rate for MRI compared to comparator imaging technique based on p-value when calculable ($P < 0.05$ all evaluations; McNemar's test).

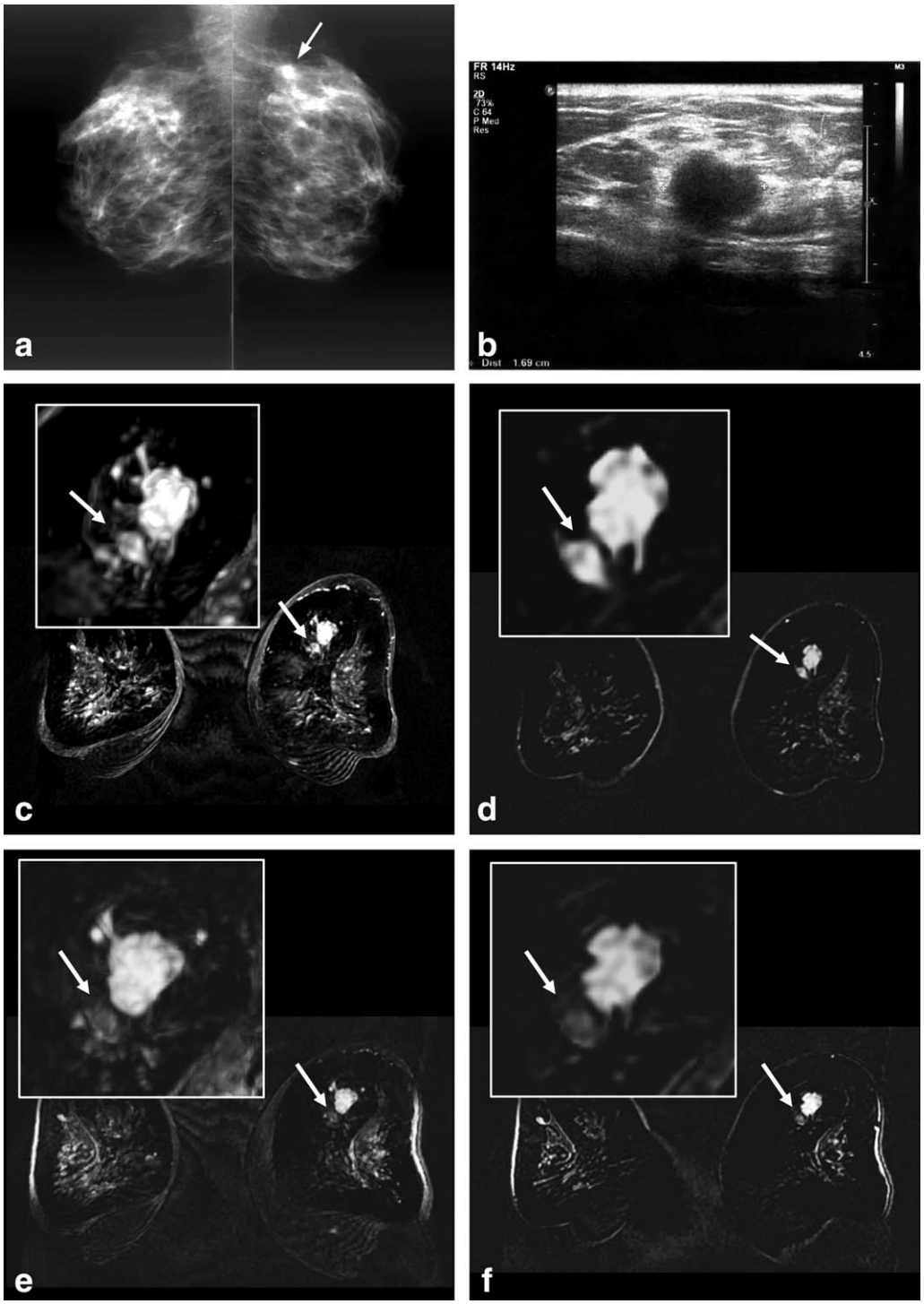

Figure 2. A 49-year-old woman undergoing breast MRI for preoperative staging. Breast tissue density: BI-RADS 3 (heterogeneously dense tissue). A single histologically proven IDC Grade III (29 mm; ER/PgR pos; HER2 neg) in the left breast (solid arrow) is visible on mammography as an irregular, spiculated, high-density mass (**a**). On ultrasound the lesion is seen as an irregular, indistinct, heterogenous, hypoechoic mass (**b**). MRI enhanced with gadobenate dimeglumine clearly depicts not only the main lesion but also a smaller satellite nodule (arrow) on both the subtracted image (**c**) and the maximum intensity projection (MIP) reconstruction (**d**). Conversely, on MRI enhanced with gadopentetate dimeglumine the smaller satellite nodule (arrow) is barely visible on the subtracted image (**e**) and only faintly visible on the MIP reconstruction (**f**). The greater lesion conspicuity and more extensive disease seen with gadobenate dimeglumine can be considered of importance for interventional planning.

on gadobenate dimeglumine-enhanced MRI that were not seen on mammography and/or ultrasound but only 13, 13 and 14 additional malignant lesions on gadopentetate dimeglumine-enhanced MRI that were not seen on mammography and/or ultrasound (Table 4). Further, gadobenate dimeglumine-enhanced MRI was more reliable at correctly characterizing additional detected lesions as malignant or benign (Table

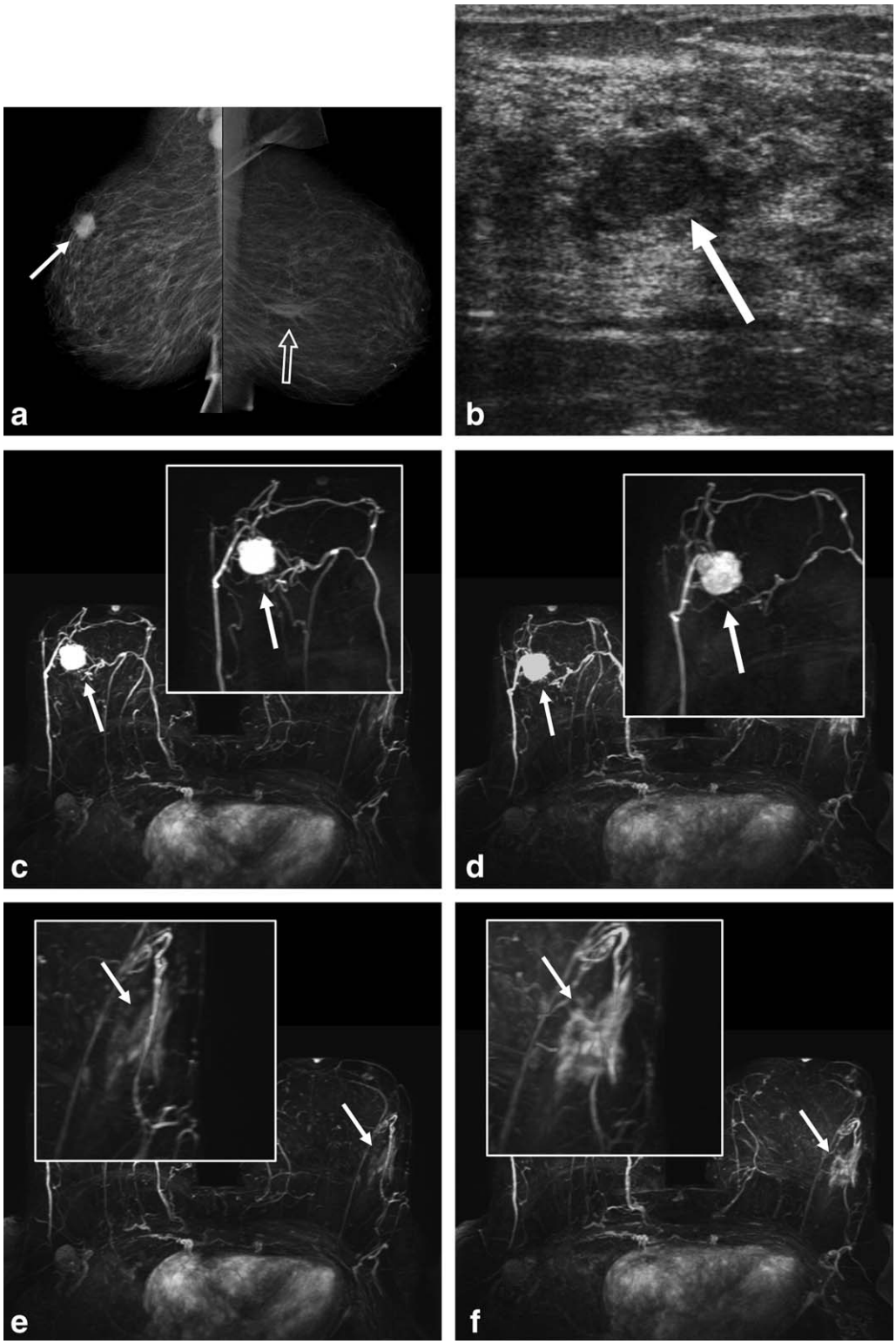

Figure 3. A 72-year-old woman undergoing breast MRI for preoperative staging. Breast tissue density: BI-RADS 1 (almost entirely fatty). A single histologically proven IDC Grade II (11–20 mm; ER/PgR neg; HER2 neg) in the right breast (solid arrow) is readily visible on mammography (**a**), ultrasound (**b**), and MRI enhanced with gadobenate dimeglumine (**c**) and gadopentetate dimeglumine (**d**). Conversely, a single ILC Grade II (>20 mm; ER/PgR neg; HER2 neg) in the left breast (open arrow) is poorly visible on mammography, was not seen on ultrasound, and is only poorly visible on gadopentetate dimeglumine-enhanced MRI (**e**). However, the lesion is clearly visible on gadobenate dimeglumine-enhanced MRI (**f**). All three readers strongly preferred gadobenate dimeglumine for all evaluations.

4). Thus, across the three blinded readers, gadobenate dimeglumine was associated with fewer FN determinations of histologically proven malignant lesions and considerably fewer FP determinations of histologically proven benign lesions. Histologically confirmed malignant lesions occult to mammography and/or

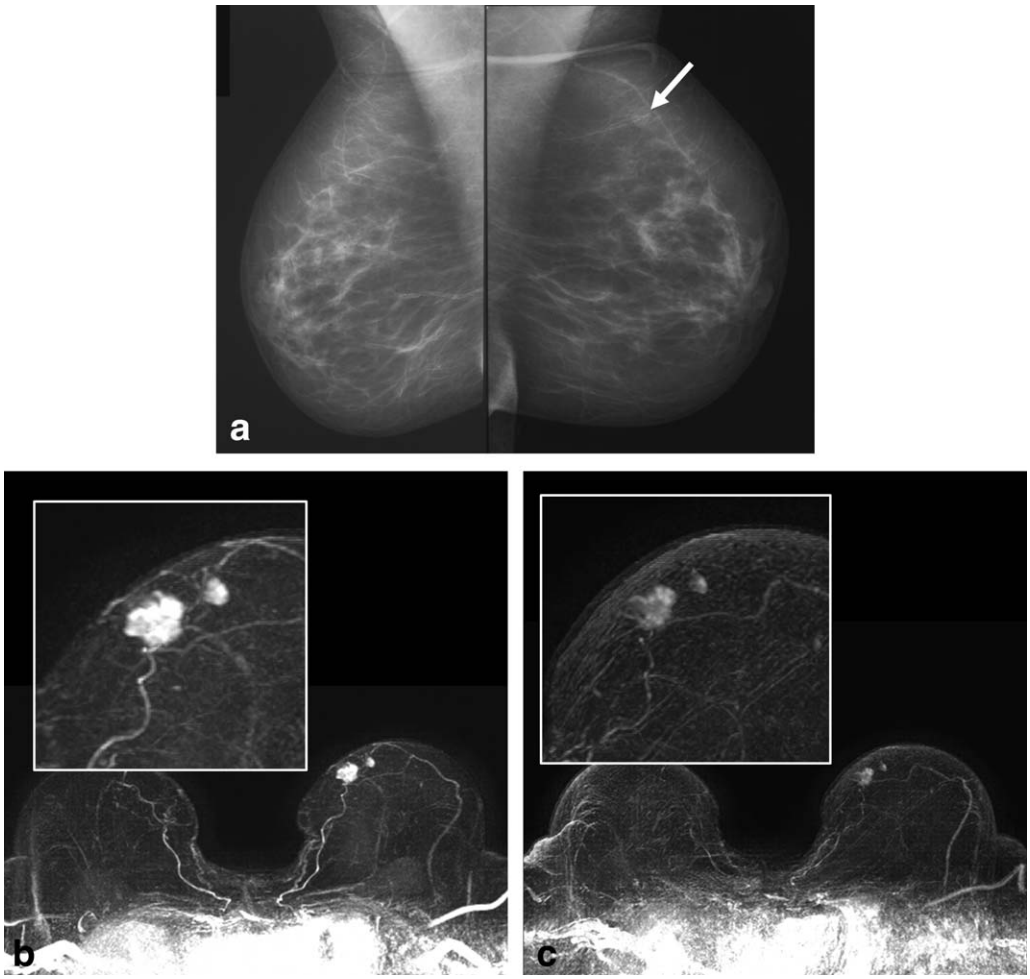

Figure 4. An 87-year-old woman undergoing breast MRI because of an indeterminate lesion on mammography and ultrasound. Breast tissue density: BI-RADS 2 (scattered islands of fibroglandular tissue). Mammography (**a**) reveals a small ill-defined lesion of low density (arrow) in the upper outer quadrant of the left breast. On ultrasound two lesions of irregular shape were identified (not shown). Subtracted MR images after gadobenate dimeglumine (**b**) and gadopentetate dimeglumine (**c**) reveal both lesions, although lesion conspicuity, enhancement, and definition are substantially better after gadobenate dimeglumine. The smaller lesion seen immediately lateral to the main lesion is considerably more conspicuous on the gadobenate dimeglumine-enhanced image and both lesions appear larger. Histopathology confirmed two IDC grade II lesions of 18 mm and 9 mm (ER/PgR pos; HER2 neg).

Table 4
Histologically Confirmed Lesions Detected by MRI But Missed at Conventional Imaging

			Additional histologically confirmed lesions detected on MRI only					
			Reader 1		Reader 2		Reader 3	
Comparator	Lesion type		Gadobenate dimeglumine	Gadopentetate dimeglumine	Gadobenate dimeglumine	Gadopentetate dimeglumine	Gadobenate dimeglumine	Gadopentetate dimeglumine
Mammography	Malignant	Total	22	18	21	17	23	19
		TP/FN	20/2	15/3	21/0	16/1	23/0	18/1
	Benign	Total	16	14	15	18	17	15
		TN/FP	14/2	10/4	12/3	11/7	16/1	9/6
Ultrasound	Malignant	Total	26	24	24	23	27	26
		TP/FN	23/3	22/2	24/0	21/2	26/1	25/1
	Benign	Total	11	11	9	11	13	10
		TN/FP	9/2	8/3	5/4	4/7	10/3	4/6
Mammography + Ultrasound	Malignant	Total	15	13	14	13	15	14
		TP/FN	14/1	12/1	14/0	12/1	15/0	13/1
	Benign	Total	10	10	8	10	11	8
		TN/FP	9/1	8/2	5/3	4/6	10/1	4/4

ultrasound which were seen on gadobenate dimeglumine-enhanced MRI but not gadopentetate dimeglumine-enhanced MRI included primarily small (2.5–13 mm) IDC and ILC. Conversely, no additional IDCs were seen on gadopentetate dimeglumine-enhanced MRI that were not also seen on gadobenate dimeglumine-enhanced MRI.

Diagnostic Performance

The diagnostic performance of breast MRI compared to mammography, ultrasound, and combined mammography and/or ultrasound is presented in Tables 5, 6, and 7, respectively. Significant ($P \leq 0.0011$) superiority for gadobenate dimeglumine-enhanced MRI versus mammography was noted by all three readers for sensitivity in diagnosing malignant disease, by one reader for specificity in diagnosing malignant disease ($P = 0.0253$), and by all three readers for accuracy in diagnosing malignant disease ($P \leq 0.0046$) (Table 5). Conversely, significant superiority for gadopentetate dimeglumine-enhanced MRI versus mammography was not noted by any reader for any parameter. Indeed, significantly lower specificity and accuracy on gadopentetate dimeglumine-enhanced MRI relative to mammography was noted by two blinded readers ($P \leq 0.016$) and one blinded reader ($P < 0.0001$), respectively. Similar findings were noted for comparisons in patients who also underwent ultrasound (Table 6) and when considering the entire population of patients who underwent mammography and/or ultrasound (Table 7). Findings for comparisons between the two MRI examinations in each patient population reflect findings reported previously (13).

Similar findings were reported for PPV and NPV for all populations. When one or more blinded readers reported a significant difference relative to the comparator technique, in all cases this reflected significantly superior PPV or NPV in the case of gadobenate dimeglumine-enhanced MRI, but significantly lower PPV or NPV in the case of gadopentetate dimeglumine-enhanced MRI.

DISCUSSION

Recently, the intraindividual comparative study "DETECT" (13) confirmed earlier studies (14,15) in showing that the detection of malignant breast lesions and the overall diagnostic performance of breast MRI is strongly influenced by the choice of MR contrast agent used for the imaging procedure. The results of the present analysis show that gadobenate dimeglumine-enhanced breast MRI is not only superior to gadopentetate dimeglumine-enhanced MRI in terms of breast cancer detection and diagnostic performance but is superior also to conventional mammography and ultrasound in terms of sensitivity, specificity, and overall accuracy. Moreover, values for PPV and NPV were in all cases higher than corresponding values for gadopentetate dimeglumine-enhanced MRI and conventional imaging techniques. In the case of PPV this indicates that the likelihood of a breast harboring malignant disease is greater if a gadobenate dimeglumine-enhanced MRI examination yields a positive result than if a comparative examination yields a positive result. Conversely, in the case of NPV the higher value indicates that the risk of overlooking malignant disease is markedly lower on gadobenate dimeglumine-enhanced MRI than on gadopentetate dimeglumine-enhanced MRI or on conventional imaging.

Of particular interest is that the cancer detection rate on gadopentetate dimeglumine-enhanced MRI was only slightly greater than that on mammography and ultrasound when these techniques were considered separately and was at best only equivalent to mammography and ultrasound in patients undergoing one or both of these techniques. There are several explanations for these findings. First, it should be borne in mind that patients were included in the study only if they had an abnormality at mammography or ultrasound that was considered BI-RADS category 3, 4, or 5 for suspicion of malignancy. Thus, given that the patients in this study were already known to have a suspicious abnormality on conventional imaging, the minimal difference in sensitivity for malignant lesion detection and diagnostic performance on gadopentetate dimeglumine-enhanced MRI can be ascribed more to the anticipated excellent performance of mammography and ultrasound than to the poor performance of gadopentetate dimeglumine-enhanced MRI. Second, MR image assessment was performed by three independent radiologists who were unaffiliated with any of the imaging centers and totally blinded to all patient clinical and radiological information that might have aided image interpretation and diagnosis. This artificial reading environment is very different from that which occurs in clinical routine and, in the case of MRI of focal liver lesions, has been shown to result in markedly poorer diagnostic performance than when reading is performed in the presence of clinical and radiological information (19). It is likely that the diagnostic performance of both gadopentetate dimeglumine- and gadobenate dimeglumine-enhanced MRI would have been improved had clinical data been available to the readers during image interpretation. Finally, and possibly less immediately intuitive, the sensitivity of gadopentetate dimeglumine-enhanced MRI will inevitably be reduced when compared to that achieved with an alternative, more sensitive technique. In this study additional, histologically confirmed malignant lesions were detected by all three blinded readers only on gadobenate dimeglumine-enhanced MRI. This will have resulted in lower sensitivities for all other techniques relative to the sensitivities which would have been obtained had these lesions remained undetected.

Importantly, the superior diagnostic performance achieved with gadobenate dimeglumine-enhanced MRI was noted by each reader for both invasive (IDC, ILC) and noninvasive (DCIS) carcinomas, and was consistent across all categories of breast tissue density. The value of gadobenate dimeglumine-enhanced MRI for breast cancer detection in women with dense breast parenchyma has been addressed previously (20). As noted elsewhere for both breast MRI (13–

Table 5
Diagnostic Performance for Detection of Malignancies on MRI Compared to Mammography: Region Level Analysis

Diagnostic performance (1080 regions)	Initial Mammography	MRI					
		Reader 1		Reader 2		Reader 3	
		Gadobenate dimeglumine	Gadopentetate dimeglumine	Gadobenate dimeglumine	Gadopentetate dimeglumine	Gadobenate dimeglumine	Gadopentetate dimeglumine
True positive (TP)	95	110	97	113	98	113	99
True negative (TN)	946	956	941	947	931	947	904
False positive (FP)	18	8	23	17	33	17	60
False negative (FN)	21	6	19	3	18	3	17
Sensitivity (%)	81.9	94.8	83.6	97.4	84.5	97.4	85.3
Difference (%)		11.2; [5.0, 17.4]; $P = 0.0008$		12.9; [6.8, 19.0]; $P = 0.0001$		12.1; [5.7, 18.5]; $P = 0.0005$	
Difference (%) vs. mammography		12.9	1.7	15.5	2.6	15.5	3.4
		[5.6, 20.3]	[–6.2, 9.6]	[8.9, 22.1]	[–5.5, 10.7]	[8.5, 22.5]	[–4.1, 11.0]
		$P = 0.0011$	$P = 0.670$	$P < 0.0001$	$P = 0.532$	$P < 0.0001$	$P = 0.371$
Specificity (%)	98.1	99.2	97.6	98.2	96.6	98.2	93.8
Difference (%)		1.6; [0.6, 2.5]; $P = 0.0011$		1.7; [0.5, 2.8]; $P = 0.0047$		4.5; [2.9, 6.0]; $P < 0.0001$	
Difference (%) vs. mammography		1.0	–0.5	0.1	–1.6	0.1	–4.4
		[0.1, 1.9]	[–1.6, 0.6]	[–1.0, 1.2]	[–2.8, –0.3]	[–0.9, 1.1]	[–5.8, –2.9]
		$P = 0.0253$	$P = 0.353$	$P = 0.847$	$P = 0.016$	$P = 0.842$	$P < 0.0001$
Accuracy (%)	96.4	98.7	96.1	98.1	95.3	98.1	92.9
Difference (%)		2.6; [1.5, 3.7]; $P < 0.0001$		2.9; [1.6, 4.1]; $P < 0.0001$		5.3; [3.7, 6.9]; $P < 0.0001$	
Difference (%) vs. mammography		2.3	–0.3	1.8	–1.1	1.8	–3.5
		[1.2, 3.5]	[–1.6, 1.0]	[0.5, 3.0]	[–2.5, 0.3]	[0.5, 3.0]	[–5.0, –2.0]
		$P < 0.0001$	$P = 0.674$	$P = 0.0046$	$P = 0.128$	$P = 0.0046$	$P < 0.0001$
PPV (%)	84.1	93.2	80.8	86.9	74.8	86.9	62.3
Difference (%)		12.4; $P < 0.0001$		12.1; $P < 0.0001$		24.7; $P < 0.0001$	
Difference (%) vs. mammography		9.1	–3.2	2.9	–9.3	2.9	–21.8
		$P = 0.0008$	$P = 0.335$	$P = 0.253$	$P = 0.0087$	$P = 0.237$	$P < 0.0001$
NPV (%)	97.8	99.4	98.0	99.7	98.1	99.7	98.2
Difference (%)		1.4; $P < 0.0001$		1.6; $P < 0.0001$		1.5; $P < 0.0001$	
Difference (%) vs. mammography		1.5	0.2	1.9	0.3	1.9	0.3
		$P < 0.0001$	$P = 0.620$	$P < 0.0001$	$P = 0.499$	$P < 0.0001$	$P = 0.416$

Includes all subjects who had all exams and histology results available.
Sensitivity = TP/(TP+FN); Specificity = TN/(TN+FP); Accuracy = (TP+TN)/(TP+TN+FP+FN);
PPV = Positive Predictive Value = TP/(TP+FP); NPV = Negative Predictive Value = TN/(TN+FN).
Values in square brackets represent 95% confidence intervals (CI). Differences and 95% CI for sensitivity, specificity and accuracy determined using paired binary approach. Significance determined using McNemar's test.
Significance of differences in PPV and NPV determined using Wald test from Generalized Estimating Equations.

Table 6
Diagnostic Performance for Detection of Malignancies on MRI Compared to Ultrasound: Region Level Analysis

Diagnostic performance (1090 regions)	Initial ultrasound	MRI					
		Reader 1		Reader 2		Reader 3	
		Gadobenate dimeglumine	Gadopentetate dimeglumine	Gadobenate dimeglumine	Gadopentetate dimeglumine	Gadobenate dimeglumine	Gadopentetate dimeglumine
True positive (TP)	93	105	91	108	92	109	96
True negative (TN)	954	963	949	954	942	946	906
False positive (FP)	22	13	27	22	34	30	70
False negative (FN)	21	9	23	6	22	5	18
Sensitivity (%)	81.6	92.1	79.8	94.7	80.7	95.6	84.2
Difference (%)		12.3; [5.8, 18.8]; $P = 0.0005$		14.0; [7.7, 20.4]; $P < 0.0001$		11.4; [4.2, 18.6]; $P = 0.0029$	
Difference (%) vs. ultrasound		10.5	–1.8	13.2	–0.9	14.0	2.6
		[3.1, 18.0]	[–10.5, 7.0]	[6.1, 20.3]	[–9.5, 7.7]	[7.2, 20.9]	[–6.0, 11.2]
		$P = 0.0073$	$P = 0.695$	$P = 0.0006$	$P = 0.842$	$P = 0.0002$	$P = 0.549$
Specificity (%)	97.7	98.7	97.2	97.7	96.5	96.9	92.8
Difference (%)		1.4; [0.5, 2.4]; $P = 0.0043$		1.2; [0.1, 2.4]; $P = 0.0339$		4.1; [2.3, 5.9]; $P < 0.0001$	
Difference (%) vs. ultrasound		0.9	–0.5	0.0	–1.2	–0.8	–4.9
		[–0.1, 2.0]	[–1.7, 0.7]	[–1.2, 1.2]	[–2.5, 0.1]	[–2.1, 0.5]	[–6.6, –3.2]
		$P = 0.0833$	$P = 0.398$	$P = 1.0$	$P = 0.064$	$P = 0.217$	$P < 0.0001$
Accuracy (%)	96.1	98.0	95.4	97.4	94.9	96.8	91.9
Difference (%)		2.6; [1.4, 3.7]; $P < 0.0001$		2.6; [1.3, 3.8]; $P < 0.0001$		4.9; [3.1, 6.6]; $P < 0.0001$	
Difference (%) vs. ultrasound		1.9	–0.6	1.4	–1.2	0.7	–4.1
		[0.7, 3.2]	[–2.0, 0.8]	[0.0, 2.7]	[–2.7, 0.3]	[–0.7, 2.1]	[–5.9, –2.4]
		$P = 0.0022$	$P = 0.370$	$P = 0.043$	$P = 0.112$	$P = 0.302$	$P < 0.0001$
PPV (%)	80.9	89.0	77.1	83.1	73.0	78.4	57.8
Difference (%)		11.9; $P < 0.0001$		10.1; $P = 0.0004$		20.6; $P < 0.0001$	
Difference (%) vs. ultrasound		8.1	–3.8	2.2	–7.9	–2.5	–23.3
		$P = 0.0069$	$P = 0.274$	$P = 0.384$	$P = 0.030$	$P = 0.678$	$P < 0.0001$
NPV (%)	97.8	99.1	97.6	99.4	97.7	99.5	98.1
Difference (%)		1.4; $P < 0.0001$		1.7; $P < 0.0001$		1.4; $P = 0.0003$	
Difference (%) vs. ultrasound		1.2	–0.2	1.5	–0.1	1.6	0.2
		$P = 0.0006$	$P = 0.602$	$P < 0.0001$	$P = 0.740$	$P < 0.0001$	$P = 0.666$

Includes all subjects who had all exams and histology results available.
Sensitivity = TP/(TP+FN); Specificity = TN/(TN+FP); Accuracy = (TP+TN)/(TP+TN+FP+FN);
PPV = Positive Predictive Value = TP/(TP+FP); NPV = Negative Predictive Value = TN/(TN+FN).
Values in brackets represent 95% confidence intervals (CI). Differences and 95% CI for sensitivity, specificity, and accuracy determined using paired binary approach. Significance determined using McNemar's test.
Significance of differences in PPV and NPV determined using Wald test from Generalized Estimating Equations.

Table 7
Diagnostic Performance for Detection of Malignancies on MRI Compared to Combined Mammography and/or Ultrasound: Region Level Analysis

		MRI					
		Reader 1		Reader 2		Reader 3	
Diagnostic performance (1310 regions)	Initial mammography and/or ultrasound	Gadobenate dimeglumine	Gadopentetate dimeglumine	Gadobenate dimeglumine	Gadopentetate dimeglumine	Gadobenate dimeglumine	Gadopentetate dimeglumine
True positive (TP)	123	127	113	131	114	132	117
True negative (TN)	1138	1160	1145	1150	1135	1141	1095
False positive (FP)	35	13	28	23	38	32	78
False negative (FN)	14	10	24	6	23	5	20
Sensitivity (%)	89.8	92.7	82.5	95.6	83.2	96.4	85.5
Difference (%)		10.2; [4.8, 15.7]; $P = 0.0005$		12.4; [6.9, 17.9]; $P < 0.0001$		10.9; [4.7, 17.2]; $P = 0.0011$	
Difference (%) vs. mammography/ultrasound		2.9	–7.3	5.8	–6.6	6.6	–4.4
		[–2.8, 8.6]	[–14.5, –0.1]	[1.0, 10.7]	[–13.6, 0.5]	[2.0, 11.2]	[–11.6, 2.9]
		$P = 0.317$	$P = 0.0499$	$P = 0.0209$	$P = 0.072$	$P = 0.0067$	$P = 0.2393$
Specificity (%)	97.0	98.9	97.6	98.0	96.8	97.3	93.4
Difference (%)		1.3; [0.4, 2.1]; $P = 0.0027$		1.3; [0.3, 2.3]; $P = 0.0112$		3.9; [2.4, 5.4]; $P < 0.0001$	
Difference (%) vs. mammography/ultrasound		1.9	0.6	1.0	–0.3	0.3	–3.7
		[0.9, 2.9]	[–0.5, 1.7]	[–0.1, 2.2]	[–1.5, 1.0]	[–0.9, 1.4]	[–5.1, –2.2]
		$P = 0.0004$	$P = 0.286$	$P = 0.0768$	$P = 0.680$	$P = 0.6744$	$P < 0.0001$
Accuracy (%)	96.3	98.2	96.0	97.8	95.3	97.2	92.5
Difference (%)		2.2; [1.3, 3.2]; $P < 0.0001$		2.4; [1.4, 3.5]; $P < 0.0001$		4.7; [3.1, 6.2]; $P < 0.0001$	
Difference (%) vs. mammography/ultrasound		2.0	–0.2	1.5	–0.9	0.9	–3.7
		[0.9, 3.1]	[–1.5, 1.0]	[0.4, 2.7]	[–2.2, 0.4]	[–0.3, 2.1]	[–5.2, –2.3]
		$P = 0.0004$	$P = 0.718$	$P = 0.0086$	$P = 0.174$	$P = 0.1275$	$P < 0.0001$
PPV (%)	77.8	90.7	80.1	85.1	75.0	80.5	60.0
Difference (%)		10.6; $P < 0.0001$		10.1; $P < 0.0001$		20.5; $P < 0.0001$	
Difference (%) vs. mammography/ultrasound		12.9	2.3	7.2	–2.8	2.6	–17.8
		$P < 0.0001$	$P = 0.553$	$P = 0.0099$	$P = 0.288$	$P = 0.291$	$P < 0.0001$
NPV (%)	98.8	99.1	97.9	99.5	98.0	99.6	98.2
Difference (%)		1.2; $P < 0.0001$		1.5; $P < 0.0001$		1.4; $P < 0.0001$	
Difference (%) vs. mammography/ultrasound		0.4	–0.8	0.7	–0.8	0.8	–0.6
		$P = 0.189$	$P = 0.0172$	$P = 0.0026$	$P = 0.0256$	$P = 0.0003$	$P = 0.1145$

Includes all subjects who had all exams and histology results available.
Sensitivity = TP/(TP+FN); Specificity = TN/(TN+FP); Accuracy = (TP+TN)/(TP+TN+FP+FN);
PPV = Positive Predictive Value = TP/(TP+FP); NPV = Negative Predictive Value = TN/(TN+FN).
Values in brackets represent 95% confidence intervals (CI). Differences and 95% CI for sensitivity, specificity, and accuracy determined using paired binary approach. Significance determined using McNemar's test.
Significance of differences in PPV and NPV determined using Wald test from Generalized Estimating Equations.

15,21) and other MRI applications (22–29) the improved diagnostic performance with gadobenate dimeglumine relative to gadopentetate dimeglumine can be ascribed to its higher R1 relaxivity (30,31), which derives from weak, transient interactions of the Gd-BOPTA contrast-effective molecule with serum albumin (32,33). Specifically, the Gd-BOPTA contrast-effective molecule of gadobenate dimeglumine, unlike the Gd-DTPA contrast-effective molecule of gadopentetate dimeglumine, possesses a hydrophobic benzyloxymethyl sidechain which is believed to fit into specific sites on the albumin molecule leading to a slowing of the tumbling rate of the gadobenate dimeglumine complex in blood and thus an increase in its relaxivity (32,33). Although the interaction with serum albumin does not influence either the plasma kinetics of gadobenate dimeglumine (34,35) or its dynamic behavior in breast MRI (13–15) relative to that seen with gadopentetate dimeglumine and other conventional gadolinium agents, the increased r1-relaxivity results in greater SI enhancement on T1-weighted images which has been shown to be of benefit for the improved detection and diagnosis of malignant lesions (13–15), for better predicting malignancy in the case of histologically borderline lesions diagnosed at core needle biopsy (36), for improved detection of malignant contralateral lesions in patients with diagnosed unilateral breast cancer (37), and for improved malignant lesion detection/exclusion and surgical decision-making in patients with breast cancer detected at conventional imaging (1). Although increased SI enhancement and correspondingly improved lesion conspicuity might also be achieved with a higher than standard dose (ie, >0.1 mmol/kg bodyweight) of gadolinium contrast agent (38), the use of higher doses is currently a matter for concern given the risk of nephrogenic systemic fibrosis, particularly in patients with severely impaired renal function.

In comparison to mammography and breast ultrasound, MRI is widely recognized as the most sensitive and appropriate diagnostic technique for the detection and diagnosis of breast cancer, particularly in women with dense breast parenchyma and in women at high genetic risk of developing breast cancer (4–11,39,40). Unfortunately, despite the numerous advantages of breast MRI in these selected patient populations, MRI is still relatively underused in clinical practice, in part because of cost and availability issues, and in part because of insufficient evidence from large-scale outcome studies (12,40). Moreover, critics suggest that breast MRI leads to more FP results and more extensive and unnecessary surgery without any improvement in surgical care or prognosis. Although our patient population comprised women considered BI-RADS category 3, 4, or 5 for suspicion of malignancy, our results suggest that improved diagnostic performance on breast MRI may be achieved if MR contrast agents with high relaxivity are used. However, it remains to be determined whether the improved malignant lesion detection rate, correspondingly reduced FP rate, and better overall diagnostic performance compared to that observed on conventional imaging and on breast MRI with standard relaxivity contrast agents translates into improved patient care and prognosis.

Possible limitations of the study are that not all patients underwent both mammography and ultrasound examinations and that blinded assessment of mammography and ultrasound images was not performed by the same three radiologists who evaluated the MR images. On the other hand, all mammography and ultrasound examinations and their subsequent evaluation were performed as routinely carried out in clinical practice by unblinded readers. A further possible limitation is that the patients included in this study were already strongly suspected of having breast cancer (BI-RADS category 3, 4, or 5 for suspicion of malignancy) based on findings from conventional imaging. As a consequence, the patient population evaluated was not entirely representative of the population that might ordinarily be referred for a breast MRI examination. On the other hand, the patients evaluated in this study included those with inconclusive findings at conventional imaging and/or those requiring breast MRI for preoperative staging, as described by the European Society of Breast Imaging (41). Further work should be directed towards assessing whether the clear benefit of gadobenate dimeglumine-enhanced MRI in this study applies to other patient populations requiring a breast MRI examination such as women at high risk for breast cancer that require routine screening MRI (39,40).

In conclusion, our data confirm that gadobenate dimeglumine-enhanced MRI is effective for breast cancer detection and diagnosis in symptomatic women referred for breast MRI and that this approach offers advantages over conventional imaging and gadopentetate dimeglumine-enhanced MRI in this patient population. The three blinded readers in our study each reported significantly better detection of malignant breast lesions on gadobenate dimeglumine-enhanced MRI compared to mammography, ultrasound, and MRI enhanced with gadopentetate dimeglumine. Improved diagnostic performance on breast MRI was noted by all three readers regardless of malignant lesion type and density of breast tissue.

REFERENCES

1. Pediconi F, Catalano C, Padula S, et al. Contrast-enhanced magnetic resonance mammography: does it affect surgical decision-making in patients with breast cancer? Breast Cancer Res Treat 2007;106:65–74.
2. Bedrosian I, Mick R, Orel SG, et al. Changes in the surgical management of patients with breast carcinoma based on preoperative magnetic resonance imaging. Cancer 2003;98:468–473.
3. Brennan ME, Houssami N, Lord S, et al. Accuracy and surgical impact of magnetic resonance imaging in breast cancer staging: systematic review and meta-analysis in detection of multifocal and multicentric cancer. J Clin Oncol 2009;27:5640–5649.
4. Warner E, Plewes DB, Shumak RS, et al. Comparison of breast magnetic resonance imaging, mammography, and ultrasound for surveillance of women at high risk for hereditary breast cancer. J Clin Oncol 2001;19:3524–3531.
5. Berg WA, Gutierrez L, NessAiver MS, et al. Diagnostic accuracy of mammography, clinical examination, US, and MR imaging in preoperative assessment of breast cancer. Radiology 2004;233:830–849.
6. Van Goethem M, Schelfout K, Dijckmans L, et al. MR mammography in the pre-operative staging of breast cancer in patients

with dense breast tissue: comparison with mammography and ultrasound. Eur Radiol 2004;14:809–816.
7. Kuhl C. The current status of breast MR imaging. Part I. Choice of technique, image interpretation, diagnostic accuracy, and transfer to clinical practice. Radiology 2007;244:356–378.
8. Warner E, Plewes DB, Hill KA, et al. Surveillance of BRCA1 and BRCA2 mutation carriers with magnetic resonance imaging, ultrasound, mammography, and clinical breast examination. JAMA 2004;292:1317–1325.
9. Kriege M, Brekelmans CT, Boetes C, et al. Efficacy of MRI and mammography for breast-cancer screening in women with a familial or genetic predisposition. N Engl J Med 2004;351:427–437.
10. Hagen AI, Kvistad KA, Maehle L, et al. Sensitivity of MRI versus conventional screening in the diagnosis of BRCA-associated breast cancer in a national prospective series. Breast 2007;16: 367–374.
11. Berg WA, Zhang Z, Cormack JB, Jong RA, Barr RG, Lehrer DE.Supplemental yield and performance characteristics of screening MRI after combined ultrasound and mammography: ACRIN 666. In: 95th Scientific Assembly and Annual Meeting, 2009, Chicago IL. Book of Abstracts; p 103.
12. Turnbull L, Brown S, Harvey I, et al. Comparative effectiveness of MRI in breast cancer (COMICE) trial: a randomized controlled trial. Lancet 2010;375:563–571.
13. Martincich L, Faivre-Pierret M, Zechmann CM, et al. Multicenter, double-blind, randomized, intraindividual crossover comparison of gadobenate dimeglumine and gadopentetate dimeglumine for breast MR imaging (DETECT Trial). Radiology 2011;258:396–408.
14. Pediconi F, Catalano C, Occhiato R, et al. Breast lesion detection and characterization at contrast-enhanced MR mammography: gadobenate dimeglumine versus gadopentetate dimeglumine. Radiology 2005;237:45–56.
15. Pediconi F, Catalano C, Padula S, et al. Contrast-enhanced MR mammography: improved lesion detection and differentiation with gadobenate dimeglumine. AJR Am J Roentgenol 2008;191: 1339–1346.
16. American College of Radiology (ACR) Breast Imaging Reporting and Data System Atlas (BI-RADS Atlas) 4th ed. Reston, VA: American College of Radiology; 2003.
17. Kuhl CK, Mielcareck P, Klaschik S, et al. Dynamic breast MR imaging: are signal intensity time course data useful for differential diagnosis of enhancing lesions? Radiology 1999;211:101–110.
18. Kuhl CK, Schild HH. Dynamic image interpretation of MRI of the breast. J Magn Reson Imaging 2000;12:965–974.
19. Hamm B, Thoeni RF, Gould RG, et al. Focal liver lesions: characterization with nonenhanced and dynamic contrast material-enhanced MR imaging. Radiology 1994;190:417–423.
20. Pediconi F, Catalano C, Roselli A, et al. The challenge of imaging dense breast parenchyma: is magnetic resonance mammography the technique of choice? A comparative study with x-ray mammography and whole-breast ultrasound. Invest Radiol 2009;44: 412–421.
21. Knopp MV, Bourne MW, Sardanelli F, et al. Gadobenate dimeglumine-enhanced MRI of the breast: analysis of dose response and comparison with gadopentetate dimeglumine. AJR Am J Roentgenol 2003;181:663–676.
22. Maravilla KR, Maldjian JA, Schmalfuss IM, et al. Contrast enhancement of central nervous system lesions: multicenter intraindividual crossover comparative study of two MR contrast agents. Radiology 2006;240:389–400.
23. Rowley HA, Scialfa G, Gao PY, et al. Contrast-enhanced MR imaging of brain lesions: a large-scale intraindividual crossover comparison of gadobenate dimeglumine versus gadodiamide. AJNR Am J Neuroradiol 2008;29:1684–1691.
24. Kuhn MJ, Picozzi P, Maldjian JA, et al. Evaluation of intraaxial enhancing brain tumors on magnetic resonance imaging: intraindividual crossover comparison of gadobenate dimeglumine and gadopentetate dimeglumine for visualization and assessment, and implications for surgical intervention. J Neurosurg 2007; 106:557–566.
25. Rumboldt Z, Rowley HA, Steinberg F, et al. Multicenter, double-blind, randomized, intraindividual crossover comparison of gadobenate dimeglumine and gadopentetate dimeglumine in MRI of the CNS at 3 Tesla. J Magn Reson Imaging 2009;29:760–767.
26. Prokop M, Schneider G, Vanzulli A, et al. Contrast-enhanced MR angiography of the renal arteries: blinded multicenter crossover comparison of gadobenate dimeglumine and gadopentetate dimeglumine. Radiology 2005;234:399–408.
27. Bültmann E, Erb G, Kirchin MA, Klose U, Naegele T. Intra-individual crossover comparison of gadobenate dimeglumine and gadopentetate dimeglumine for contrast-enhanced MR angiography of the supraaortic vessels at 3 Tesla. Invest Radiol 2008;43: 695–702.
28. Gerretsen S, le Maire T, Miller S, et al. Multicenter, double-blind, randomized, intraindividual crossover comparison of gadobenate dimeglumine and gadopentetate dimeglumine for MR angiography of the peripheral arteries. Radiology 2010;255:988–1000.
29. Schneider G, Maas R, Schultze Kool L, et al. Low-dose gadobenate dimeglumine versus standard dose gadopentetate dimeglumine for contrast-enhanced magnetic resonance imaging of the liver: an intra-individual crossover comparison. Invest Radiol 2003;38:85–94.
30. Rohrer M, Bauer H, Mintorovitch J, Requardt M, Weinmann HJ. Comparison of magnetic properties of MRI contrast media solutions at different magnetic field strengths. Invest Radiol 2005;40: 715–724.
31. Pintaske J, Martirosian P, Graf H, et al. Relaxivity of gadopentetate dimeglumine (Magnevist), gadobutrol (Gadovist), and gadobenate dimeglumine (MultiHance) in human blood plasma at 0.2, 1.5, and 3 Tesla. Invest Radiol 2006;41:213–221 (erratum, Invest Radiol 2006;41:859).
32. Cavagna FM, Maggioni F, Castelli PM, et al. Gadolinium chelates with weak binding to serum proteins. A new class of high-efficiency, general purpose contrast agents for magnetic resonance imaging. Invest Radiol 1997;32:780–796.
33. Giesel FL, von Tengg-Kobligk H, Wilkinson ID, et al. Influence of human serum albumin on longitudinal and transverse relaxation rates (R1 and R2) of magnetic resonance contrast agents. Invest Radiol 2006;41:222–228.
34. Spinazzi A, Lorusso V, Pirovano G, Taroni P, Kirchin M, Davies A. MultiHance clinical pharmacology: biodistribution and MR enhancement of the liver. Acad Radiol 1998;5:S86–S89.
35. Spinazzi A, Lorusso V, Pirovano G, Kirchin M. Safety, tolerance, biodistribution and MR imaging enhancement of the liver with gadobenate dimeglumine. Acad Radiol 1999;6:282–291.
36. Pediconi F, Padula S, Dominelli V, et al. Role of breast MR imaging for predicting malignancy of histologically borderline lesions diagnosed at core needle biopsy: prospective evaluation. Radiology 2010;257:653–661.
37. Pediconi F, Catalano C, Roselli A, et al. Contrast-enhanced MR mammography for evaluation of the contralateral breast in patients with diagnosed unilateral breast cancer or high-risk lesions. Radiology 2007;243:670–680.
38. Heywang-Köbrunner SH, Haustein J, Pohl C, et al. Contrast-enhanced MR imaging of the breast: comparison of two different doses of gadopentetate dimeglumine. Radiology 1994;191:639–646.
39. Lee CH, Dershaw DD, Kopans D, et al. Breast cancer screening with imaging: recommendations from the Society of Breast Imaging and the ACR on the use of mammography, breast MRI, breast ultrasound, and other technologies for the detection of clinically occult breast cancer. J Am Coll Radiol 2010;7:18–27.
40. Saslow D, Boetes C, Burke W, et al. American Cancer Society guidelines for breast screening with MRI as an adjunct to mammography. CA Cancer J Clin 2007;57:75–89.
41. Mann RM, Kuhl CK, Kinkel K, Boetes C. Breast MRI: guidelines from the European Society of Breast Imaging. Eur Radiol 2008; 18:1307–1318.